Structural Studies on Transmembrane Proteins. 2. Spin Labeling of Bacteriorhodopsin Mutants at Unique Cysteines†

Christian Altenbach,‡ Sabine L. Flitsch,§,∥ H. Gobind Khorana,§ and Wayne L. Hubbell*,‡

Jules Stein Eye Institute and Department of Chemistry and Biochemistry, University of California, Los Angeles, Los Angeles, California 90024-1771, and Departments of Biology and Chemistry, Massachusetts Institute of Technology, 77 Massachusetts Avenue, Cambridge, Massachusetts 02139

Received February 9, 1989; Revised Manuscript Received June 1, 1989

ABSTRACT: Site-directed mutagenesis was used to produce mutants of bacteriorhodopsin where either glycine-72, threonine-90, leucine-92, or serine-169 was replaced by a cysteine. Two different spin labels were then covalently attached to these sites. The selection of attachment sites covered two postulated loops (72, 169) and a membrane-spanning segment (90, 92). It was not possible to properly refold the protein labeled at position 90, presumably due to steric problems, but the EPR spectra of the other mutants that were successfully reconstituted in phospholipid vesicles provided information on the dynamics of protein side chains in the vicinity of the label site. A power saturation approach was used to investigate the spin relaxation times, which in turn can be influenced by collisions with paramagnetic species. The differential effect of oxygen and a water-soluble chromium complex on the power-saturation behavior of the spin-labeled mutants was used to obtain topographical information on the sites in the membrane-bound protein. The results are consistent with residues 72 and 169 being located in structured loops exposed to the aqueous phase and residue 92 being localized in the membrane interior, possibly near a helix–helix contact region.

Transmembrane proteins form a very important class and the solution of their structure–function relationship on a molecular level is of great interest. Crystallographic methods have been very successful in solving the three-dimensional structure of soluble proteins, but so far the only good three-dimensional crystals obtained from a transmembrane protein have been for the photosynthetic reaction center II (Deisenhofer et al., 1985). Besides, the static structure does not provide direct information about dynamic structural changes during functional operation.

The spin-labeling technique [see Berliner (1976, 1979) and Dalton (1985) for comprehensive monographs] is capable of providing structural and dynamic information in macromolecules, but the lack of suitably located reactive sites on a protein, where a spin label can be selectively attached, has prevented general application to proteins. Recently, methods have been developed to overcome the three major difficulties: sensitivity, selectivity, and versatility. Sensitivity is required to work with the limited amounts of material often available, selectivity to attach the label at only one unique single protein site, and versatility to select this site at any position in the protein sequence. The introduction of loop–gap resonator technology essentially solved the sensitivity problem for small aqueous samples (Froncisz & Hyde, 1982). For example, it is now routinely possible for usable single-scan spectra to be obtained with as little as 10 pmol of protein. Recent technological advances in other areas have provided solutions to the selectivity and versatility problems. For small proteins, high-resolution chromatographic methods allow separation of a randomly labeled mixture into fractions, each containing only one label at unique site. Taken together, the fractions provide proteins selectively labeled at multiple locations that can be used to extract global structural information. This approach was successful with the bee venom protein melittin (Altenbach & Hubbell, 1988).

For larger proteins, a very promising approach is to use site-directed mutagenesis to replace any amino acid of a protein, one at a time, with a suitable attachment site for a spin label. This approach has recently been used to study regions of colicin E1 by introduction of cysteines in selected regions of the protein, followed by spin labeling with cysteine-specific nitroxides (Todd et al., 1987).

Recently, several cysteine mutants of bacteriorhodopsin have been successfully expressed, functionally reconstituted, and biochemically characterized as described in detail in the preceding paper (Flitsch & Khorana, 1989). The locations of the introduced cysteines were selected to maximize the number of clearly different environments: position 72 is believed to be in an extracellular small loop, position 169 in a larger intracellular loop, and positions 90 and 92 on opposite faces of a membrane-spanning α-helix (Figure 1). Figure 1 of the preceding paper (Flitsch & Khorana, 1989) shows their locations in a proposed secondary structure. Here we describe the spin labeling of these mutants and show how EPR[1] spectroscopic methods can be used to obtain topographical and dynamical information. A preliminary report on this work has been presented (Altenbach et al., 1989).

Conventional EPR spectroscopy yields information about the motional state and environment of the attached spin label. In a protein, this is a complex function of the neighboring side chains and solvent molecules, the structure of the attached spin label, and hydrogen-bonding interactions between spin label and protein. Taking advantage of these spectral sensitivities, it is possible to draw inferences regarding side-chain packing and polarity of the immediate environment of a spin label in

† Supported by Grant EY05216 from the National Institutes of Health and the Jules Stein Professor endowment to W.L.H. S.L.F. is a recipient of Deutscher Akademischer Austauschdienst Grant 1985–1987.

‡ University of California, Los Angeles.

§ Massachusetts Institute of Technology.

∥ Present address: Chemistry Department, University of Exeter, Stocker Road, Exeter EX4 4QD, U.K.

[1] Abbreviations: bR, bacteriorhodopsin; CROX, potassium chromium oxalate (potassium trioxalatochromate); CW, continuous wave; ELDOR, electron–electron double resonance; EPR, electron paramagnetic resonance; SDS, sodium dodecyl sulfate.

0006-2960/89/0428-7806$01.50/0

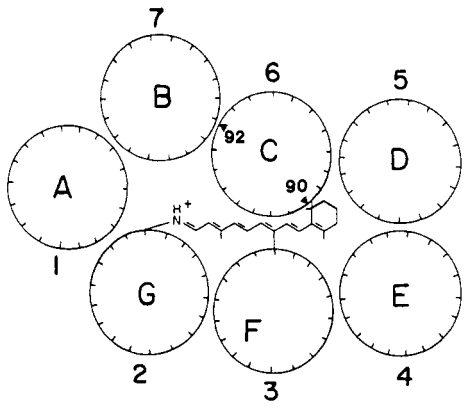

FIGURE 1: Top view of the proposed membrane structure of bacteriorhodopsin [modified from Khorana (1988)]. Helix C is rotated by ~+20° to reflect the results of this study. The inclusion of the chromophore is for the purpose of orientation and does not necessarily reflect the correct retinal conformation or geometry relative to the protein. The tilt of helices A, G, and F is not shown.

a protein. If a sequential series of cysteine mutants is available, it is also possible in favorable cases to deduce the local secondary structure from the periodicity of spectral properties (Todd et al., 1987). Of course, time-dependent changes in these features can also be followed (Hubbell et al., 1987), making the approach ideal for study of conformational changes.

Site-directed spin labels can also be used to investigate topography of a membrane protein, i.e., whether a particular residue is located in the membrane interior or in either of the two aqueous phases bounding the membrane. The primary tool in exploring membrane protein topograpy is spin exchange [see Molin et al. (1980) for the definitive treatment of the subject]. Spin exchange results from the direct collision of a paramagnetic species with the nitroxide, an event that is readily detected experimentally. It is thus possible to determine whether a nitroxide at a particular site on a protein is within the membrane interior or in the aqueous phase simply by determining the exchange frequency in the presence of a lipid or water-soluble paramagnetic exchange reagent. This phase-specific spin exchange has been employed earlier in the study of melittin conformation at membrane surfaces (Altenbach & Hubbell, 1988; Altenbach et al., 1988).

Chromium oxalate (CROX) is an excellent choice for a water-soluble exchange reagent (Berg & Nesbitt, 1979; Yager et al., 1979). It is highly insoluble in the membrane interior and will undergo exchange only with nitroxides exposed to the aqueous phase. It has a charge of −1 to −2 in the physiological pH range and should be employed in the presence of a moderate ionic strength to minimize electrostatic effects. It is relatively bulky, and the collision frequency is strongly affected by steric interactions in the local environment around the nitroxide.

Molecular oxygen is an outstanding exchange reagent that has solubility in both the membrane interior and aqueous solutions, although it prefers hydrocarbon phases to water by about 10 to 1 in concentration (Wilhelm & Battino, 1973; Wilhelm et al., 1977). It has a very small molecular volume and is less affected by steric constraints than chromium oxalate. If a spin label on a protein does not undergo exchange with oxygen, it is safe to conclude that it is buried in a compact domain.

Spin exchange with a fast relaxing paramagnetic species like O_2 and CROX results in changes in both T_{1e} and T_{2e} electron relaxation times of a nitroxide spin label, and measurement of these parameters provides a direct means of estimating collision frequencies. Changes in T_{1e} can be determined by pulse saturation recovery EPR spectroscopy (Hyde, 1979; Subczynski et al., 1987; Altenbach et al., 1988). Continuous wave (CW) power saturation techniques are sensitive to the $T_{1e}T_{2e}$ product (Castner, 1959; Poole & Farach, 1971; Poole, 1983). Changes in T_{2e} can be estimated from changes in line width. However, measurement of direct line broadening is feasible only for very high collision frequencies since the effects are small, especially if the spin label is motionally restricted.

In the present paper, we apply CROX, O_2, and the CW power saturation approach to investigate the locations of two different spin labels attached to Cys-72, Cys-92, and Cys-169 of the bR mutants. In addition, several interesting conclusions derived from the mobility of the nitroxide side chains are discussed.

The loop–gap resonator technology mentioned above greatly facilitates the determination of power saturation effects in two ways. First, very high values of the microwave magnetic field component can be attained at the sample by using standard klystrons without amplification. This permits the study of relatively short relaxation times with simple instrumentation. Second, the microwave magnetic field is very homogeneous over the sample volume, greatly simplifying the analysis.

THEORY

Power Saturation Method of T_{1e} Determination. For a single homogeneous Lorentzian line the peak-to-peak amplitude of the first derivative absorption spectrum, Y', has the form (Poole, 1983)

$$Y' \propto H_1/(1 + H_1^2\gamma^2T_{1e}T_{2e})^{1.5} \quad (1)$$

where H_1 is the microwave magnetic field component in gauss, γ is the gyromagnetic ratio of the electron, and T_{1e} and T_{2e} are the spin–lattice and spin–spin relaxation times, respectively. In a microwave resonator, H_1 is proportional to the square root of the incident microwave power, P

$$H_1 = \Lambda P^{1/2} \quad (2)$$

where Λ is a constant depending on the properties of the resonator.

From (1) and (2) it can be seen that at very low power the signal *increases* as $P^{1/2}$, whereas at high power it *decreases* as $1/P$. The system is said to saturate when the amplitude begins to deviate from the square root dependency on power. Saturation is due to an inability of the spin system to relax to equilibrium at a rate competitive with that at which power is absorbed from the microwave field. The rate of relaxation to equilibrium with the lattice is measured by $1/T_{1e}$. Thus, a sample with a long T_{1e} has a slow relaxation rate and saturates easily, and one with a short T_{1e} saturates with difficulty. An easily extractable parameter to describe this saturation behavior of a sample is $P_{1/2}$ (Subczynski & Hyde, 1981). This is the microwave power required to saturate the signal to half the amplitude it would have if it did not saturate at all.

From (1) and (2) above, it is readily shown that $P_{1/2}$ is proportional to $1/(T_{1e}T_{2e})$:

$$P_{1/2} = (2^{2/3} - 1)/(\Lambda^2\gamma^2T_{1e}T_{2e}) \quad (3)$$

Thus, determination of $P_{1/2}$ provides a means of estimating the $T_{1e}T_{2e}$ product.

Effect of Paramagnetic Species. Collision of a nitroxide with a fast-relaxing paramagnetic species results in spin exchange and an increase of the nitroxide relaxation rate $1/T_{1e}$ in proportion to the collision frequency

$$\frac{1}{T_{1e}} - \frac{1}{T_{1e}^0} = fp\omega_e \quad (4)$$

Scheme I

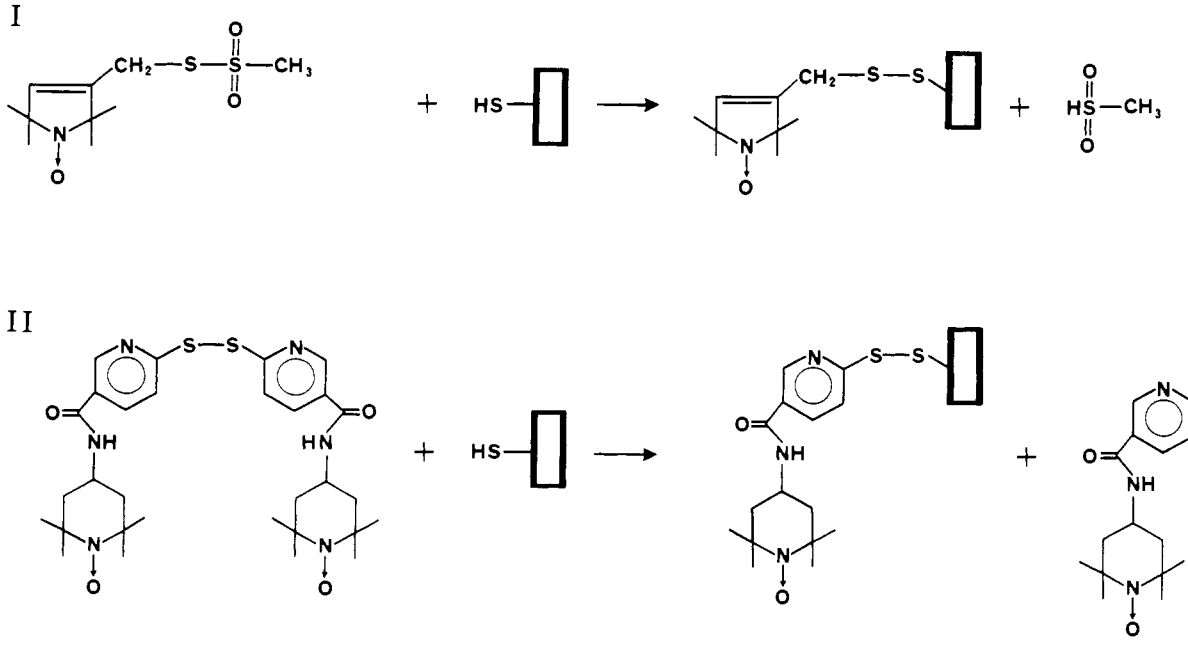

where ω_e is the collision frequency, f is a statistical factor (Subczynski & Hyde, 1981), p is the collision efficiency, and $1/T_{1e}^0$ is the relaxation rate in the absence of a relaxing agent.

From (3) and (4), it can be deduced that the change in $P_{1/2}$ due to the presence of a relaxing agent is proportional to the collision frequency

$$\Delta P_{1/2} = P_{1/2} - P_{1/2}^0 \propto \frac{1}{T_{1e}T_{2e}} - \frac{1}{T_{1e}^0 T_{2e}^0} \sim\propto \frac{\omega_e}{T_{2e}^0} \qquad (5)$$

Since $1/T_{2e}$ is usually much faster than the collision rate, T_{2e} is not significantly affected by the collisions and is a constant. For different spin labels with comparable T_{2e}, $\Delta P_{1/2}$ reflects the relative collision frequency and therefore accessibility. If, however, the spin labels have significantly different T_{2e}, the one with the shorter T_{2e} will have a larger $\Delta P_{1/2}$ for the same accessibility.

Since T_{1e} for nitroxides is on the order of a microsecond, significant effects of relaxing agent on $P_{1/2}$ require a collision frequency on the order of megahertz.

The above discussion has assumed a single homogeneous Lorentzian line. Nitroxide line shapes are not this simple, and (3) cannot be reliably used to determine absolute values of relaxation times for these species. In addition, the relaxation times estimated from CW saturation methods are *effective* relaxation times since they are affected by nitrogen nuclear relaxation rates (Hyde & Sarna, 1978; Subczynski & Hyde, 1981). However, *changes* in $P_{1/2}$ due to the presence of an exchange reagent reflect parallel changes in T_{1e} due to collisions (Hyde & Sarna, 1978; Subczynski & Hyde, 1981; Vachon et al., 1987).

Materials and Methods

Reagents. The methanethiosulfonate spin label I [*S*-(1-oxy-2,2,5,5-tetramethylpyrroline-3-methyl) methanethiosulfonate] was obtained from Reanal (Budapest, Hungary). The pyridine disulfide spin label II [2,2′-dithiobis[5-[[(1-oxy-2,2,6,6-tetramethylpiperidin-4-yl)amino]carbonyl]-pyridine]] was prepared in one step by the coupling of 2,2′-dithiodinicotinic acid and tempamine (Aldrich Chemical Co., Milwaukee, WI) with isobutyl chloroformate in anhydrous DMF according to the method of Wieland and Bernhard (1951). Chromium oxalate (potassium trioxalatochromate) was obtained from ICN Pharmaceuticals (Plainview, NY). Tempone was obtained from Aldrich.

Spin Labeling of Bacteriorhodopsin. The bacteriorhodopsin mutants were prepared as described in the preceding paper (Flitsch & Khorana, 1989). Spin labeling was performed prior to folding and reconstitution. Scheme I shows the chemical reaction and structures of the two spin labels employed.

Typically, mutant bacteriorhodopsin (0.08 mM) in 6 M urea, 3% SDS, 0.1 M sodium phosphate, pH 7, 10 mM ethylenediaminetetraacetic acid, and 0.05% sodium azide was incubated with 0.16 mM dithiothreitol for 1 h at 37 °C. Label I or II was added in acetonitrile to give a final concentration of 3.8 or 9 mM, respectively. The mixture was then incubated for 2 h at room temperature. After dialysis (1 day, two buffer changes) against 10 mM sodium phosphate, pH 6, 0.2% sodium dodecyl sulfate, and 0.05% sodium azide, the chromophore was regenerated with *all-trans*-retinal in detergent/phospholipid micelles (Flitsch & Khorana, 1989). The regenerated samples were further purified by size exclusion chromatography to remove unregenerated protein and reconstituted into asolectin vesicles (Flitsch & Khorana, 1989) containing a lipid to protein ratio of 40:1 by weight. Purified bR labeled at positions 72, 92, and 169 had absorption spectra typical of normal bR, with an A_{280}/A_{546} ratio of 1.6–1.8, a value characteristic of the pure chromophore (Flitsch & Khorana, 1989). bR labeled at position 90 could not be regenerated. As a control, the labeling procedures were also performed on wild-type bR which contains no cysteine. No EPR signal could be detected under these conditions. From the integrated EPR signal and the known concentration of bR, the number of spins per bR could be estimated and was close to unity in all cases.

Measurement and Analysis of Conventional EPR Spectra. A Varian E-109 EPR spectrometer (Varian Associates Inc., Palo Alto, CA) operating at X-band and fitted with a two-loop one-gap resonator (Hubbell et al., 1987) and interfaced to a Nicolet 1280 computer (Nicolet Instrument Corp., Madison, WI) was used. To provide stable AFC lock with this configuration, the microwave bridge was modified, as described elsewhere (Hubbell et al., 1987). The gas-permeable TPX plastic sample capillary (Wilmad Glass Co., Inc., Buena, NJ) had an active volume of approximately 1 μL.

Rotational correlation times for label I were estimated by matching positions of the hyperfine extrema of the spectra to those of a library of spectra simulated for isotropic motion. The simulation program used was developed by Freed and co-workers and generously provided by that group (Freed, 1976). No attempt was made at complete spectral simulation for the present study, since the spectra apparently reflect a distribution of motional states; rotational correlation times were estimated only for the extremes of the distribution.

Measurements and Analysis of Saturation Curves. To obtain meaningful saturation curves in the absence and presence of CROX, all traces of oxygen must be removed from the sample. For that purpose, the sample capillary was fabricated from gas-permeable TPX plastic and continuously surrounded by flowing nitrogen gas during the measurements (Popp & Hyde, 1981). For oxygen-exchange experiments, nitrogen gas was replaced by oxygen. The $M_I = 0$ resonance line was usually scanned over 10–20 G as a function of microwave power in the range 0.1–200-mW input power. For the loop–gap resonator, this corresponds to a microwave magnetic field (H_1) of 0.045–2 G. To obtain a saturation curve, the peak-to-peak amplitude of the first derivative spectrum was measured and plotted against the square root of microwave power. The data were fit to an equation containing two terms of the form of (1), each with adjustable initial slope and $\gamma^2 T_{1e} T_{2e}$ parameter. The $P_{1/2}$ values were determined from the curve as the intersection point with a straight line that has half the initial slope of the saturation curve.

Measurement of the Permeability of the Reconstituted Vesicles to Chromium Oxalate. Tempone (1 mM) spin label and 50 mM chromium oxalate were added to the reconstituted membranes. Tempone readily crosses the membrane and distributes homogeneously, but chromium oxalate completely broadens the tempone spectrum only on the outside of the vesicle (Vistnes & Puskin, 1981). A sharp residual tempone spectrum results from tempone inside the vesicles which cannot collide with chromium oxalate. The amplitude of this residual spectrum is proportional to the vesicle internal volume, and its disappearance over time would indicate chromium oxalate leaking into the vesicle interior.

Results and Discussion

Both spin labels employed in this study react exclusively with free sulfhydryl groups. Label I, based on the alkyl alkanethiosulfonates pioneered by Kenyon and co-workers (Bruice & Kenyon, 1977) and first prepared by Berliner et al. (1982), is particularly useful for the present purposes. It is extremely reactive under mild conditions and has a relatively small molar volume, similar to that of a phenylalanine residue. Thus, it introduces a minimal structural perturbation in the protein. However, in certain cases even this cannot be tolerated (see below). In addition, once attached to the protein it has only weak hydrogen-bonding capacity to interact with nearby groups in the protein. This is important if one wishes to study the dynamics of the radical in the structure to determine steric constraints imposed by the environment. If the motion of the nitroxide side chain is limited by hydrogen bonding, little could be concluded regarding pure steric interactions. Label II is based on the pyridine disulfide sulfhydryl reagent introduced by Grassetti and Murray (1967). This label is of larger physical size than I and has hydrogen-bonding capacity conferred by the amide linkage. The nitroxide is separated from the reactive functionality by more bonds than in I and in principle can give rise to a large range of motions in an unrestricted environment.

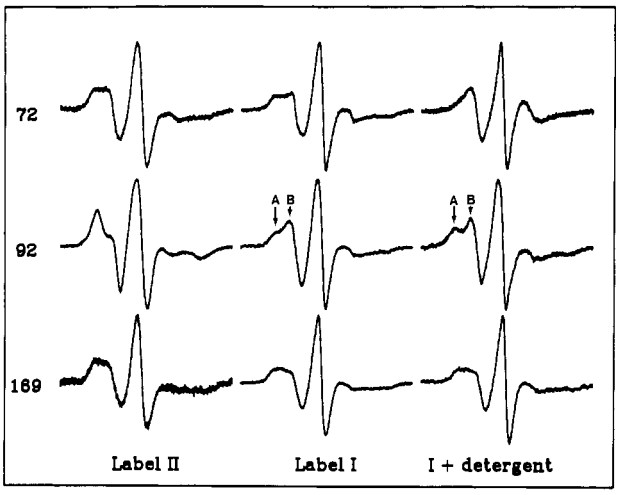

FIGURE 2: Comparison of the EPR spectra of the spin-labeled bR mutants reconstituted in asolectin vesicles. The bacteriorhodopsin mutants were labeled with the pyridine disulfide spin label II (left) or methanethiosulfonate spin label I (center and right). The spin label was attached either to position 70, 92, or 169 as indicated on the left. At right, the effect of solubilization in 1% octyl glucoside is shown. The scan range is 100 G. The sample contained typically 100–200 pmol of labeled protein.

Each mutant reacted quantitatively with the spin labels in the unfolded state in SDS/urea solution. Consistent with the findings of the preceding paper (Flitsch & Khorana, 1989), Thr-90 → Cys does not refold when the spin labels are attached. Both spin labels have a molar volume significantly larger than threonine, and presumably steric constraints prevent proper folding. Gly-72 → Cys, Leu-92 → Cys, and Ser-169 → Cys all refolded and regenerated the typical bR-like chromophore after labeling with either I or II.

The conclusions of this work are based primarily on results obtained with spin label I, and these are discussed below for each of the mutants. A characteristic feature of all spectra of I on membrane-bound bR is that they apparently represent multiple populations differing in mobility of the nitroxide side chain relative to the protein. Consider, for example, the spectrum of I on Cys-92 (Figure 2). In this case, two clearly identifiable populations are evident, marked by arrows in the figure. The broader of the spectral components [(A) in the figure] corresponds to a correlation time of about 50 ns, while the other more mobile component [(B) in the figure] has a correlation time on the order of 20 ns. The two populations could arise from two different conformations of an individual bR exchanging slowly on the EPR time scale or two different conformations of the spin label on the protein. We cannot logically distinguish between the two. Since the regenerated, labeled, bR was pure as judged by the A_{280}/A_{546} ratio, there is no reason to believe that the two populations are folded and unfolded forms. Two conformations of the label on a given protein would not be surprising, since the disulfide bond linking the label to the protein can exist in two conformations with a barrier on the order of 10–20 kcal between them (Jocelyn, 1972). At 10 kcal, the interconversion rate would be on the order of megahertz, which is slow on the EPR time scale, and separate spectral populations would be observed. It is less likely that the two populations arise from intermolecular interactions of bR (monomer ⇔ trimer equilibrium, for example), since bR has been found to be monomeric above a molar protein to lipid ratio of 1:40. In addition, bR solubilized in octyl glucoside shows two populations (Figure 2) and has also been found to be monomeric in this detergent (Heyn & Dencher, 1982).

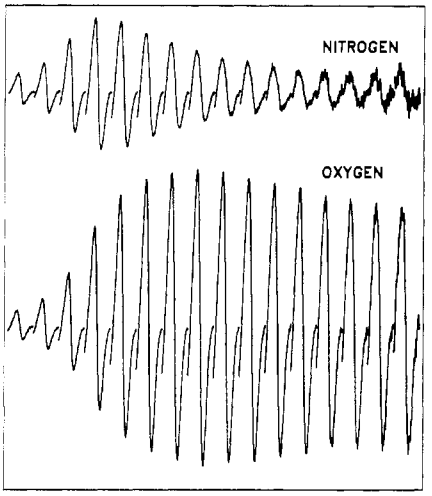

FIGURE 3: Saturation behavior for reconstituted bacteriorhodopsin labeled at position 169 with methanethiosulfonate spin label I. (Top) Under nitrogen (i.e., in the absence of any paramagnetic relaxing agent); (bottom) the identical sample equilibrated with 100% oxygen gas at atmospheric pressure measured. The center line was scanned over 20 G at the following power settings (left to right): 0.1, 0.25, 1, 4, 9, 16, 25, 36, 49, 64, 81, 100, 121, 144, 169, and 196 mW. All other machine parameters, including gain, were held constant. The noise level increases as a function of microwave power. The identical signal amplitude at low power with and without oxygen indicates that T_{2e} is not significantly affected by the relaxing agent. At high microwave power, the presence of oxygen leads to a much increased amplitude because the shorter T_{1e} relaxation time reduces the saturation of the signal.

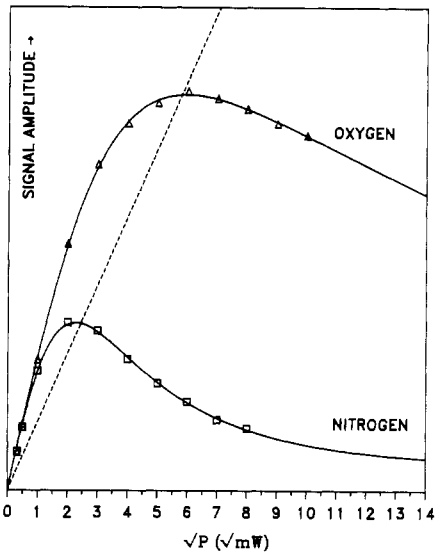

FIGURE 4: Example of two typical saturation curves extracted from the data in Figure 3. The x axis is the square root of the incident microwave power (which is proportional to the H_1 microwave magnetic field in gauss), and the y axis is the peak to peak amplitude of the first derivative EPR signal of the center line in arbitrary units. The solid line shows the theoretical curves as obtained from a nonlinear least-squares analysis of the data (see text). The dashed line has half the initial slope of the saturation curves and intersects each saturation curve at a value corresponding to the square root of $P_{1/2}$. The $P_{1/2}$ values are 6.0 and 33.5 mW, respectively, and $\Delta P_{1/2}$ = 27.5 mW.

The accessibility of the nitroxide group on each of the mutants for collision with oxygen and CROX was investigated with the CW power saturation method described above. As an example of the data, Figure 3 shows the amplitude of the $M_I = 0$ resonance line of spin label I attached to Cys-169 as a function of microwave power in the presence and absence of oxygen. The saturation of the signal and the effect of oxygen are evident. Figure 4 shows the power saturation curves determined from the data in Figure 3. The $P_{1/2}$ value is the intersection of the dotted straight line with the saturation curve, and the increase in this parameter reflects the effect of spin exchange between oxygen and the nitroxide group. For each of the mutants in both membranes and detergent, similar curves were obtained for oxygen and CROX, and the *changes* in $P_{1/2}$ due to the relaxing reagent were determined. These values are summarized in Table I and discussed below.

CROX is a charged species and is expected to be membrane impermeable. This was confirmed for the bR-containing vesicles used in these experiments by the tempone/CROX exchange approach discussed under Materials and Methods. The result is that CROX in the extravesicular solution did not significantly enter the bR vesicles even after 21 h at room temperature. However, when the sample is freeze–thawed twice by cooling to −20 °C for 5 min, CROX was completely equilibrated. Experiments with CROX were thus carried out both before and after freeze–thawing to ensure accessibility to the vesicle inner surface. Conclusions regarding group accessibility to CROX are based on changes in $P_{1/2}$ after freeze–thaw treatment (Table I).

Consider now label I on Cys-92. The $P_{1/2}$ is shifted to higher powers in the presence of oxygen, indicating a collision frequency of O_2 with the nitroxide on the order of megahertz (see Theory). Calhoun et al. (1988) have measured the rate constant for collisional quenching of tryptophan phosphorescence by O_2 in a number of proteins. For truly buried tryptophans, they find rate constants on the order of 10^6 Hz/M.

Table I: $\Delta P_{1/2}$ Parameters for Spin-Labeled bR Derivatives under Different Conditions[a]

(A) $\Delta P_{1/2} = P_{1/2} - P_{1/2}^0$ in mW for Spin-Labeled Bacteriorhodopsin in Vesicles

	label site					
	72–I	92–I	169–I	72–II	92–II	169–II
100% oxygen	21.37	43.74	27.51	19.52	17.26	15.28
50 mM CROX	3.14	1.68	13.57	3.25	1.10	2.78[b]
50 mM CROX F/T[c]	4.78	*b*	30.53	10.37	2.84	*b*

(B) $\Delta P_{1/2} = P_{1/2} - P_{1/2}^0$ for Spin-Labeled Bacteriorhodopsin in 1% Octyl Glucoside

	label site		
	72–I	92–I	169–I
100% oxygen	35.43	26.32	51.64
50 mM CROX	84.73	1.81	55.20
50 mM CROX + 100% oxygen	159.19	28.90	165.86

[a] This is the $P_{1/2}$ relative to the value in the absence of relaxing agent ($P_{1/2}^0$). A larger number indicates increased accessibility to the relaxing agent. ($P_{1/2}^0$ was very similar under all conditions: $P_{1/2}^0$ = 6.22 ± 0.26 mW). The label site is identified by the residue number and the spin-label type. I indicates the methanethiosulfonate spin label and II the pyridine disulfide spin label. [b] Not measured or very low S/N. [c] After four freeze–thaw cycles.

The local concentration of O_2 in a hydrocarbon phase in equilibrium with pure O_2 in the gas phase at atmospheric pressure is about 12 mM (Wilhelm & Battino, 1973). The expected effective collision frequency of O_2 with buried tryptophans is then about 1.2×10^4 Hz. The actual collision frequency (measured in the ESR experiment) could be as much as 9 times higher or $\sim 10^5$ Hz (Calhoun et al., 1988). This is much smaller than observed for label I at Cys-92. Thus, the nitroxide on Cys-92 experiences a collision frequency with O_2 significantly greater than a buried residue.

According to the model for bR in the membrane shown in Figure 1 of the preceding paper (Flitsch & Khorana, 1989), Cys-92 should be located on helix C near the center of membrane. An intramembrane location is supported by the con-

trasting effects of CROX and O_2 on $P_{1/2}$ in both the membrane and detergent solutions. CROX, a charged, hydrophilic paramagnetic species, has a very small effect on $P_{1/2}$, while the effect of the more hydrophobic reagent O_2 is substantial as just discussed. When the membranes are solubilized in octyl glucoside, these relative accessibilities to CROX and O_2 are maintained, as expected if the 92 region is incorporated in the hydrophobic interior of a micelle. $\Delta P_{1/2}$ is about 44 mW for nitroxide I on cysteine-92 (Table I). The $\Delta P_{1/2}$ values observed for this nitroxide on proteins within the membrane interior under the same conditions employed here range from $\simeq$30 to 140 mW (unpublished results); residue 92 is thus only moderately accessible to oxygen. One possible explanation is that it may be located near or at a contact face between helices as suggested by the model in Figure 1. This conclusion is consistent with results reported in the previous paper which show that a large label attached to Cys-92 prevents proper folding (Flitsch & Khorana, 1989). An interesting observation is that the proportion of the more mobile population decreases upon dissolution of the membrane in octyl glucoside (Figure 2, right-hand column) accompanied by a decrease in oxygen accessibility.

Cys-72 and Cys-169 are located in putative loop regions in the extracellular and intracellular aqueous phases, respectively [Figure 1 of the preceding paper (Flitsch & Khorana, 1989)]. The spectrum of label I attached to these residues has not been simulated satisfactorily with motional models of a single spin population and appears to represent a distribution of states. Nevertheless, a major contribution is quite immobilized with a correlation time on the order of 200 ns. Again, the multiple populations may be due to rotamers about various bonds, including the disulfide bond or protein domain motions slow on the EPR time scale. The most interesting result is the low mobility of the nitroxide side chain. Todd et al. (1987) have shown that label I attached to cysteine residues on the exposed surface of a putative helix in colicin E1 exhibits rapid anisotropic motion. Thus, bond isomerizatons in the side chain are of a sufficient rate to produce motional averaging of the nitroxide magnetic parameters. The slow motion of the nitroxide side chain at Cys-72 and Cys-169 is then the result of direct interaction with other side chains. Whatever structure is responsible for this interaction has a long lifetime (at least 200 ns) and argues in favor of a highly structured region in the neighborhood of these residues rather than a mobile loop. This is in agreement with deuterium NMR results that find only highly restricted motions of phenylalanine residues in bR [there are phenylalanines in both putative loops containing residues 169 and 72 (Herzfeld et al., 1987)].

Cys-72 is sufficiently exposed to the aqueous phase in the folded, membrane-bound protein to react with the hydrophilic reagent iodoacetic acid (Flitsch & Khorana, 1989). Nevertheless, label I attached to Cys-72 experiences a low collision frequency with CROX in the membrane-bound state (see Table I). This is certainly due in part to electrostatic interactions with the nearby Glu-74 and the negative surface potential in asolectin vesicles (CROX has a net negative charge between −1 and −2) as well as steric constraints. When the protein is solubilized in octyl glucoside, the motional rate of the nitroxide side chain *increases* dramatically, and the nitroxide becomes highly exposed to collision with CROX (Table I). Apparently, solubilization has removed local constraints that restricted both motion and access in the membrane. The motional changes are due to modulation of steric factors, such as local unfolding of the polypeptide. The accessibility changes to CROX could involve electrostatic interaction as well. Taken together, these results indicate that solubilization in octyl glucoside leads to changes in the hydrophobic domains near Cys-92 as well as in the putative loop region containing Cys-72. Assuming that solubilization of bR in octyl glucoside does not lead to *major* structural rearrangements, the results also permit the conclusion that Cys-72 must be at or near the aqueous phase.

Cys-169 is relatively exposed to collision with chromium oxalate in the membrane, demonstrating a location in contact with the aqueous phase consistent with the model in Figure 1 of the preceding paper (Flitsch & Khorana, 1989). Upon solubilization in octyl glucoside, very little change in mobility occurs. Thus, whatever changes in packing occur in the hydrophobic domain, they are not propagated to this putative loop region.

In spin-labeling studies of this kind, it is important to employ more than one label of reasonably different structure to assess whether the conclusions determined are due to specific features of the label or specific features of the protein environment. With this in mind, many of the experiments were repeated with the disulfide label II. To the extent that they can be compared, the conclusions are similar to those derived from the more extensive studies with label I. Label II at Cys-92 shows isotropic motion with a single component (see Figure 2) with correlation time about 30 ns. The motion is a bit faster than for I presumably due to an additional bond between the attachment point and the nitroxide. As with label I at Cys-92, it is exposed to collision with O_2, but not with CROX. Label II attached to either Cys-72 or Cys-169 shows highly restricted motion in the same time domain as label I, further supporting the conclusion of highly structured regions in the neighborhood of these residues. Nitroxide II at either position is not particularly accessible to CROX and only moderately accessible to O_2. Experiments in octyl glucoside were not carried out with this label.

Summary and Conclusions

In summary, the primary conclusions from the above studies are the following: (1) Cys-92 is located in the membrane interior, at a location in the bR molecule moderately accessible to collision with O_2. (2) Both Cys-72 and Cys-169 are located in regions in or near the aqueous phase bounding the membrane. (3) Cys-72 and Cys-169 are located in ordered domains that have lifetimes of at least 200 ns. This indicates that the regions containing residues 72 and 169 are not highly flexible. (4) Upon solubilization in octyl glucoside, significant structural changes occur in the regions of Cys-92 and Cys-72, but not near Cys-169. (5) The above conclusions are consistent with the topology of sites proposed in the model of Figures 1 of this and the preceding paper (Flitsch & Khorana, 1989).

The studies reported here indicate the utility of site-directed mutagenesis to provide spin-label attachment sites. In principle, information on topology, structure, and dynamics can be obtained at any point in a protein for which a functional X → Cys mutation can be expressed. In the present work, we have used only conventional spectroscopy in the frequency domain to obtain information. With the availability of the loop–gap resonator, more sophisticated techniques such as ELDOR and pulse saturation recovery can be employed to extract another dimension of information on topology and dynamics in labeled proteins with high sensitivity for small samples. The real time resolution of existing EPR instrumentation makes it possible to follow conformational changes on the time scale of the bR photocycle. It is then possible, with a sufficient number of mutants, to map out the conformationally active regions of the molecule during pumping. The

use of double X → Cys mutations will make it possible to introduce two spin systems in protein. Interactions between spins will then allow proximity relations between specific points to be determined. Studies to exploit these features are currently under way.

References

Altenbach, C., & Hubbell, W. L. (1988) *Proteins: Struct., Funct., Genet. 3*, 230–242.

Altenbach, C., Froncisz, W., Hubbell, W. L., & Hyde, J. S. (1988) *Biophys. J. 53*, 94a.

Altenbach, C., Flitsch, S., Khorana, H. G., & Hubbell, W. L. (1989) *J. Cell. Biochem. Suppl. 13a*, 50.

Berg, S. P., & Nesbitt, D. M. (1979) *Biochim. Biophys. Acta 548*, 608–615.

Berliner, L. J., Ed. (1976) *Spin Labeling Theory and Applications*, Academic Press, New York.

Berliner, L. J., Ed. (1979) *Spin Labeling Theory and Applications II*, Academic Press, New York.

Berliner, L. J., Grünwald, J., Hankovszky, H. O., & Hideg, K. (1982) *Anal. Biochem. 119*, 450.

Bruice, T. W., & Kenyon, J. L. (1982) *J. Protein Chem. 1*, 47–58.

Calhoun, D. B., Englander, S. W., Wright, W. W., & Vanderkooi, J. M. (1988) *Biochemistry 27*, 8466–8474.

Castner, T. G. (1959) *Phys. Rev. 115*, 1506–1515.

Dalton, L. R., Ed. (1985) *EPR and Advanced EPR Studies of Biological Systems*, CRC Press, Boca Raton.

Deisenhofer, J., Epp, O., Miki, K., Huber, R., & Michel, H. (1985) *Nature 318*, 618–624.

Flitsch, S. L., & Khorana, H. G. (1989) *Biochemistry* (preceding paper in this issue).

Freed, J. H. (1976) in *Spin Labeling Theory and Applications* (Berliner, L. J., Ed.) pp 53–161, Academic Press, New York.

Froncisz, W., & Hyde, J. S. (1982) *J. Magn. Reson. 47*, 515–521.

Grassetti, D. R., & Murray, J. F. (1967) *Arch. Biochem. Biophys. 119*, 41–49.

Herzfeld, J., Mulliken, C. M., Siminovitch, D. J., & Griffin, R. G. (1987) *Biophys. J. 52*, 855–858.

Heyn, M. P., & Dencher, N. A. (1982) *Methods Enzymol. 88*, 31–35.

Hubbell, W. L., Froncisz, W., & Hyde, J. S. (1987) *Rev. Sci. Instrum. 58*, 1879–1886.

Hyde, J. S. (1979) in *Time Domain Electron Spin Resonance* (Kevin, L., & Schwartz, R. M., Eds.) pp 1–30, Wiley, New York.

Jocelyn, P. C. (1972) *Biochemistry of the SH Group*, Academic Press, London.

Khorana, H. G. (1988) *J. Biol. Chem. 263*, 7439–7442.

Molin, Y. N., Salikhov, K. M., & Zamaraev, K. I. (1980) *Springer Ser. Chem. Phys. 8*.

Poole, C. P. (1983) *Electron Spin Resonance*, Wiley, New York.

Poole, C. P., & Farach, H. A. (1971) *Relaxation in Magnetic Resonance*, Academic Press, New York.

Popp, C. A., & Hyde, J. S. (1981) *J. Magn. Reson. 43*, 249–258.

Subczynski, W. K., & Hyde, J. S. (1981) *Biochim. Biophys. Acta 643*, 283–291.

Subczynski, W. K., Antholine, W. E., Hyde, J. S., & Peterling, D. H. (1987) *J. Am. Chem. Soc. 109*, 46–52.

Todd, A. P., Crozel, V., Levinthal, F., Levinthal, C., & Hubbell, W. L. (1987) *Biophys. J. 51*, 83a.

Vachon, A., Lecomte, C., Berleur, F., Roman, V., Fatome, M., & Braquet, P. (1987) *J. Chem. Soc., Faraday Trans. 1 83*, 177–190.

Vistnes, A. I., & Puskin, J. S. (1981) *Biochim. Biophys. Acta 644*, 244–250.

Wieland, T., & Bernhard, H. (1951) *Ann. Chem. 572*, 190.

Wilhelm, E., & Battino, R. (1973) *Chem. Rev. 73*, 1–9.

Wilhelm, E., Battino, R., & Wilcock, J. (1977) *Chem. Rev. 77*, 219–262.

Yager, T. D., Eaton, G. R., & Eaton, S. S. (1979) *Inorg. Chem. 18*, 725–727.